



Confinement of reinforced concrete columns by means of carbon-FRCM jackets

Flora Faleschini^{a,b}, Mariano Angelo Zanini^a, Lorenzo Hofer^a, Carlo Pellegrino^a

^a *Dipartimento di Ingegneria Civile, Edile e Ambientale, Via Francesco Marzolo 9, 35121 Padova, Italy*

^b *Dipartimento di Ingegneria Industriale, Via Gradenigo 6, 35121 Padova, Italy.*

Keywords: FRCM; carbon fibers; reinforced concrete column; confinement.

ABSTRACT

The rehabilitation of existing reinforced concrete (RC) elements through jacketing technique has become widely-diffused practice, that allows members to attain both strength gain and, in most cases, ductility improvement, if compared to the original element. Such positive structural behavior is permitted by concrete confinement, that can be obtained for instance by both fiber reinforced polymer (FRP) or fiber reinforced cementitious matrix (FRCM) composites use. Here, the results of an experimental campaign aimed at studying the axial behavior of reinforced concrete columns confined with FRCM are shown. A carbon-based composite was used, that includes a balanced bidirectional carbon sheets embedded in a single-component fiber-reinforced cementitious matrix. Carbon sheets were used in 1 or 2 layers. The study involves the realization of twelve 1m-height columns, having two cross-section geometries, i.e. circle and square, this latter with rounded corner radius. Among the test specimens, eight were confined with carbon-FRCM (CFRCM) and four were left as control, without any external jacket. Additionally, two stirrups spacings were adopted, as a further investigation variable. Results were lastly analyzed in terms of stress vs. axial strain response, stirrup steel reinforcement and fiber hoop strains development.

1 INTRODUCTION

In recent years, intensive research has been carried out to study fiber reinforced cementitious matrix composites (FRCM) composites, for improving the flexural, shear, and axial capacity of existing concrete members (Triantafillou and Papanicolaou 2005; Pellegrino and D'Antino 2013; Tetta and Bournas 2016). FRCM composites are comprised of high strength fibers in the form of open-mesh configuration, and ordinary cement mortars, which is typically modified by adding mineral additions and polymers. Such technology is considered as an alternative of the well-known fiber reinforced polymer (FRP) one, which generally displays lower efficiency of its counterpart, but at the same time, provides some positive features such as the possibility of applying it on wet surfaces, a better compatibility with the substrate, higher fire resistance, and nonetheless, it is cheaper.

Concerning axial confinement of reinforced concrete (RC) members, applying the FRCM

jackets along the height of the elements has been shown to enhance the axial strength and also ductility of the confined member, with respect to the unconfined case. One of the first studies on this subject (Triantafillou et al. 2006) analyzed plane concrete cylinders confined with carbon FRCM jackets, which were then tested monotonically under axial load. Results highlighted how carbon FRCM jackets were able to attain an increased peak axial strength, which ranged between 25% and 77%, depending on the applied number of fiber layers and on the tensile strength of the cementitious matrix. Further on, De Caso y Basalo et al. (2012) studied the influence of external reinforcement on glass-FRCM confined concrete cylinders, focusing on the influence of the number of fibers layer. The higher number of layers used (four in this case), the higher was the strength gain attained by the specimens. Colajanni et al. (2014a) studied instead the axial behaviour of PBO-FRCM confined concrete elements, having both square and circular cross-sections. They obtained an increase in the axial strength and ductility for the type of geometries, although lower in the former

than in the latter. For these latter, they found that the increase in axial strength was proportional not only to the number of layers, but also to the overlapping length and the mechanical properties of the matrix. This work also highlighted a relevant influence of the overlapping length. Concerning the behaviour under cyclic axial loads, for carbon-FRCM confined specimens tested, it was found that before the peak load, the envelope of axial load vs. strain curve is equal to that found under monotonical loading. However, the same does not occur after the peak load, because the cyclic load curve is lower (Colajanni et al., 2014b).

As briefly shown before, many studies have been carried out in literature on the topic of axial performance of FRCM-confined concrete members, but most of them related to small-scale concrete specimens, with limited slenderness and absence of internal steel reinforcement. Hence, this study focuses on FRCM-confined RC members, aiming to improve the knowledge on such jacketing system applied on near-full scale elements.

2 EXPERIMENTAL CAMPAIGN

Twelve RC columns were casted and tested under uniaxial compressive loading at the Laboratory for Construction Materials Tests of the University of Padova. Among them, four RC columns were plain (unconfined) and eight of them were confined by means of carbon-FRCM jackets. The variables that were investigated during this research are: geometry of column cross-section; spacing of transverse reinforcement; number of fiber layers. Table 1 summarizes the features of each column.

Table 1. Specimens ID and main features.

ID	Cross-section geometry	Stirrups spacing	No. layers
C20-0	Circular	$s_1 = 200$ mm	0
S20-0	Square	$s_1 = 200$ mm	0
C33-0	Circular	$s_2 = 330$ mm	0
S33-0	Square	$s_2 = 330$ mm	0
C20-1	Circular	$s_1 = 200$ mm	1
C20-2	Circular	$s_1 = 200$ mm	2
S20-1	Square	$s_1 = 200$ mm	1
S20-2	Square	$s_1 = 200$ mm	2
C33-1	Circular	$s_2 = 330$ mm	1
C33-2	Circular	$s_2 = 330$ mm	2
S33-1	Square	$s_2 = 330$ mm	1
S33-2	Square	$s_2 = 330$ mm	2

Two-cross sections geometry were chosen: a circular one (diameter $d = 30$ cm) and a square one (size $b = 30$ cm), with rounded section edges (corner radius $r = 2$ cm). Columns height was equal to $h = 100$ cm; concrete cover was set equal to $c = 2$ cm. Concerning steel reinforcement, Figure 1 shows the details of longitudinal reinforcement and stirrups arrangement. Recall that two different transverse reinforcement configurations, namely $s_1 = 330$ mm and $s_2 = 200$ mm, are used along the length of the columns. These reinforcing details are typical of RC columns designed prior to current seismic codes, as well as in constructions where the columns are designed to carry gravity load only.

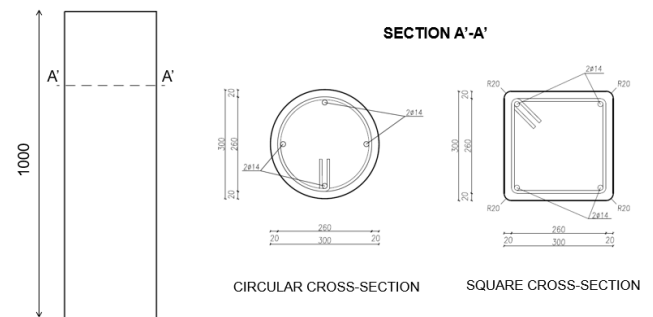


Figure 1. Column geometry and reinforcement arrangement.

2.1 Materials

Concerning materials property, all specimens were realized with a single low-strength concrete batch. The aim of this choice, i.e. that of using a relatively low strength concrete target, is to simulate a situation typically encountered when dealing with old structures that require retrofit interventions. The same aim has driven the choice of using the stirrups configuration labelled with the term s_1 . Hence, average concrete properties evaluated after 28 days from concrete casting on a sufficient number of cylinder specimens cured in the same maturation conditions of those applied to the column samples, revealed the following experimental properties: compressive strength $f_c = 21.6 \pm 3.35$ MPa, tensile strength $f_{ct} = 1.12 \pm 0.18$ MPa, elastic modulus $E_c = 26.2 \pm 2.40$ GPa.

A B450C steel type was adopted for the reinforcement. The following experimental material properties were assessed through a sufficient number of tensile strength tests, on respectively 14mm and 8mm bars: yielding strength $f_y = 552$ MPa at a strain value of $\epsilon_y = 0.002$; ultimate tensile strength $f_t = 650$ MPa at ϵ_t

$= 0.009$; $f_{yw} = 485$ MPa at $\varepsilon_y = 0.002$, $f_{tw} = 630$ MPa at $\varepsilon_{tw} = 0.009$.

As regards the carbon-FRCM system, a commercially available carbon-based composite was used, which is realized with balanced bidirectional carbon sheets embedded in a fiber-reinforced cementitious matrix. The properties of the carbon fiber, declared by the producer and integrated with proper experimental tests, are: overall area weight $W = 170$ g/m², fiber elastic modulus $E_f = 242$ GPa, fiber tensile strength $f_u = 1487$ (MPa) at ultimate tensile strain $\varepsilon_{fu} = 1.1\%$, equivalent nominal thickness $t_f = 0.047$ mm, confinement reinforcement ratio $\rho_f = 0.0025$, axial rigidity of the composite $\rho_f E_f = 0.605$ GPa. The mortar, provided by the same producer, was a premixed single-component low modulus fiber-reinforced matrix, with polymeric and inorganic binders having pozzolanic property. The properties of the mortar were experimentally evaluated at the time of each column testing, these being: flexural strength $f_{fm} = 5.67 \pm 0.65$ MPa, and compressive strength $f_{cm} = 31.9 \pm 2.4$ MPa.

2.2 Strengthening operations

The following procedure was performed:

1. Initially damping of concrete surface, to homogeneously hydrate the concrete support.
2. Application of the first layer of mortar was applied onto the surface, with an average thickness of 3 mm.
3. Application of the first layer of fibers onto the mortar surface, gentle pushing it to adhere well with the matrix.
4. Application of the new layer of mortar and carbon fiber.

Recall that steps 3 and 4 were re-done in case of two fiber layers application. The overlapping length of the fiber was set equal to 20 cm.

2.3 Testing protocol and instrumentation

Tests were carried out following a displacement-control protocol for the axial load application, with a loading speed of 0.3mm/min. Ultimate conditions were conventionally assumed at a load drop of 20% of the maximum value achieved by each specimen. Axial strains and transverse strains in the fiber and steel hoop bars were monitored during all the test, through the following instrumentation:

- axial strain: a couple of electrical strain gages were applied at column mid-height in two opposite faces (gauge length of 6 cm); three/four mechanical strain gages mounted on the external surface of the specimen, at column mid-height (gauge length of 25 cm); two linear voltage displacement transducers (LVDTs) to measure the movement of the plate mounted at the column top (gauge length = the entire length of the column).
- transverse strain in the steel and fiber reinforcement: four electrical strain gages applied onto the central stirrup at the column mid-height before concreting; two electrical strain gages per each fiber layer.

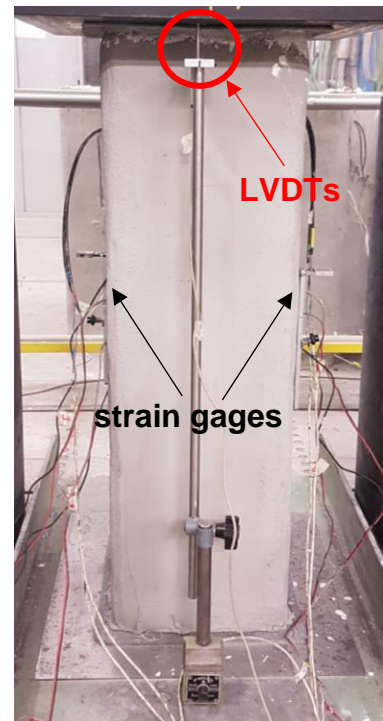


Figure 2. Disposition of instrumentation for axial strain evaluation.

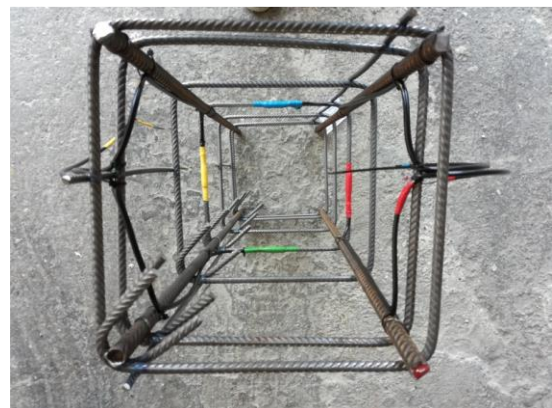


Figure 3. Disposition of instrumentation for transverse steel strain evaluation.

Figure 2 shows the disposition of the instrumentation for evaluating the axial strain, whereas Figure 3 shows how strain gages were disposed on hoop bars.

3 RESULTS AND DISCUSSION

Results for unconfined and confined specimens are discussed in this section, based on the following experimental parameters: concrete axial strength f_{c0} and f_{cc} at the load peak, f_{cu0} and f_{cu} at the ultimate load (i.e., at a drop of the maximum applied load of 20%), for the unconfined and confined specimens, respectively; axial strain ϵ_{c0} and ϵ_{cc} at the load peak, ϵ_{cu0} and ϵ_{cu} at the ultimate load, for the unconfined and confined specimens, respectively. Table 2 lists the above mentioned parameters for the analyzed columns

Table 2. Main results.

ID	f_{c0} or f_{cc} (MPa)	f_{cu0} or f_{cu} (MPa)	ϵ_{c0} or ϵ_{cc} (‰)	ϵ_{cu0} or ϵ_{cu} (‰)
C20-0	21.2	17.0	3.2	6.6
S20-0	21.1	16.9	2.7	5.5
C33-0	18.1	14.5	1.8	3.5
S33-0	17.1	13.7	3.2	4.4
C20-1	23.0	18.4	4.2	7.7
C20-2	26.2	21.0	5.0	8.4
S20-1	20.3	16.2	3.8	7.5
S20-2	21.2	17.0	4.0	7.5
C33-1	19.8*	15.8	2.8*	6.0
C33-2	21.9	17.5	4.5	7.5
S33-1	17.1	13.7	2.3	5.6
S33-2	20.9	16.7	3.2	4.2

* f_{cc} and ϵ_{cc} value here refers to the first peak (see the stress-strain curve in Figure 6).

3.1 Unconfined columns

The best performance, both in terms of axial strength gain and strain development, among the unconfined columns was attained by those specimens having the lowest stirrup spacing value, i.e. $s_l = 200\text{mm}$. No significant discrepancies (about 1%) were observed for these specimens between the two geometries. Instead, such difference increases up to 6% between the square and circular cross-section geometry for the specimens realized with the highest stirrups spacing (i.e., $s_2 = 330\text{ mm}$). Additionally, in this latter case, the performance is significantly lower, with a reduction of about -20% in the f_{cc} term if compared with the samples realized with the highest shear reinforcement ratio. Results in terms of attained load P and observed axial strains are

shown in Figure 4, where the pre-peak branch was obtained through the measurements recorded by the mechanical strain gages applied onto concrete specimens, whereas the post-peak branch through the LVDTs. Instead, for the axial strain, only the S33-0 column displayed lower ductility than the other specimens, as a result of a less efficient confinement mechanism provided by the internal steel reinforcement, in the square geometry configuration.

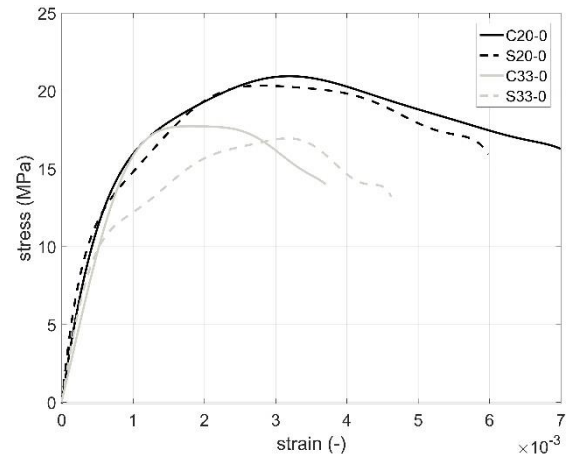


Figure 4. Stress-axial strain curve for unconfined columns.

Concerning transverse strains in the central stirrup, it is worth to cite that only those specimens having the highest transverse reinforcement spacing (i.e., $s_2 = 330\text{ mm}$) displayed the yielding of the central stirrup, that occurred, as expected, after the peak stress achievement. Such result is highlighted in Figure 5.

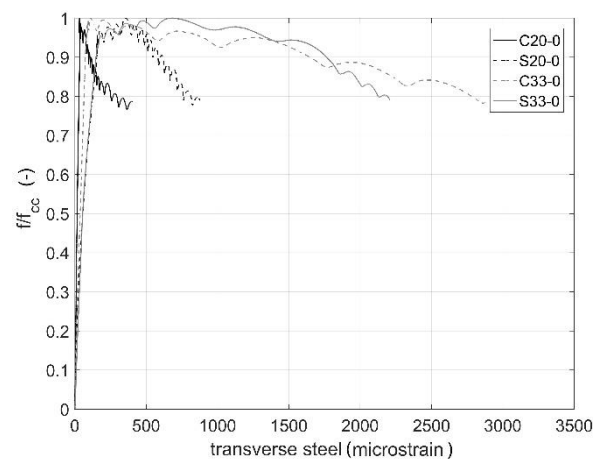


Figure 5. Dimensionless stress-transverse steel strain curve for unconfined columns.

3.2 Confined columns

Stress-axial strain curves for confined columns are shown in Figure 6. There, specimens jacketed with one fiber layer are shown with continuous

lines, whereas those having two layers are represented with dotted lines. The same instrumentation used for unconfined specimens was used to evaluate the pre- and post-peak branches.

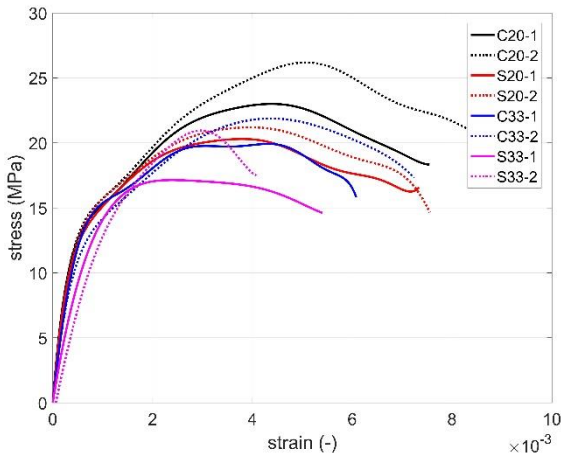


Figure 6. Stress-axial strain curve for confined columns.

A positive contribution linked to the increase of fiber layers number is observed, as peak strength is always highest in specimens with two fiber layers. Additionally, in all cases except for S33-2 column, the ultimate strain is enhanced, where a premature failure occurred linked to high concentration development of stress at one edge, with the formation of a remarkable cracking pattern (see Figure 7).



Figure 7. Cracks pattern development at the rounded edge with $r = 20$ mm (S33-2 specimen).

The best result in terms of confined concrete strength development is achieved by C20-2 column as expected, which has a circular cross-section geometry. Additionally, this specimen is characterized by the lowest stirrup spacing and it was strengthened by two fiber layers.

As concerns axial strains, ultimate values significantly depend on both stirrups spacing and on the number of fiber layers. Additionally, cross-section geometry affects the results too, being the worst behavior that of square columns. Such result confirms the recent result of the authors on small-scale specimens (Gonzalez-Libreros et al. 2019), who highlighted how a corner radius $r = 20$ mm is insufficient for ensuring the proper exploitation of the carbon-FRCM jacket in members with square geometry and 150mm side.

Instead, looking at transverse strains in the central stirrup, only the S33-1 and S33-2 columns displayed yielding. Recall that such specimens present the square geometry and the highest stirrups spacing. In all the other cases, the strains remain lower than the yielding limit, and in some cases these values were particularly low, as in the case of circular geometry with lowest stirrups spacing. Figure 8 shows the results in terms of f/f_{cc} ratio against transverse strain.

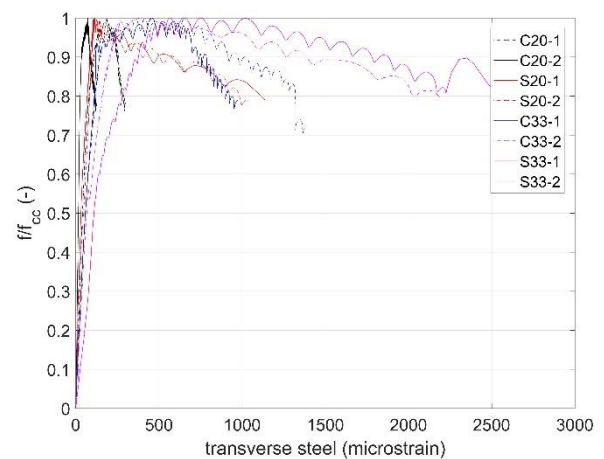


Figure 8. Dimensionless stress-transverse steel strain curve for confined columns.

Lastly, as concerns the local behavior, here the strains development in the fibers jacket were monitored through a pair of electrical strain gage per each layer. As a consequence, it was possible to assess how each jacketing configuration was able to exploit the confining action on the test samples. Particularly, the results for specimens C33-2 and S33-2 are shown in Figures 9a and 9b, respectively. SG7f and SG8f (where present) refer to the first layer, whereas SG9f and SG10f to the second layer. There, it is possible to observe how the circular cross-section geometry allows the development of higher deformation of the fibers, in contrast of the square cross-section one, where the strains observed are much more limited.

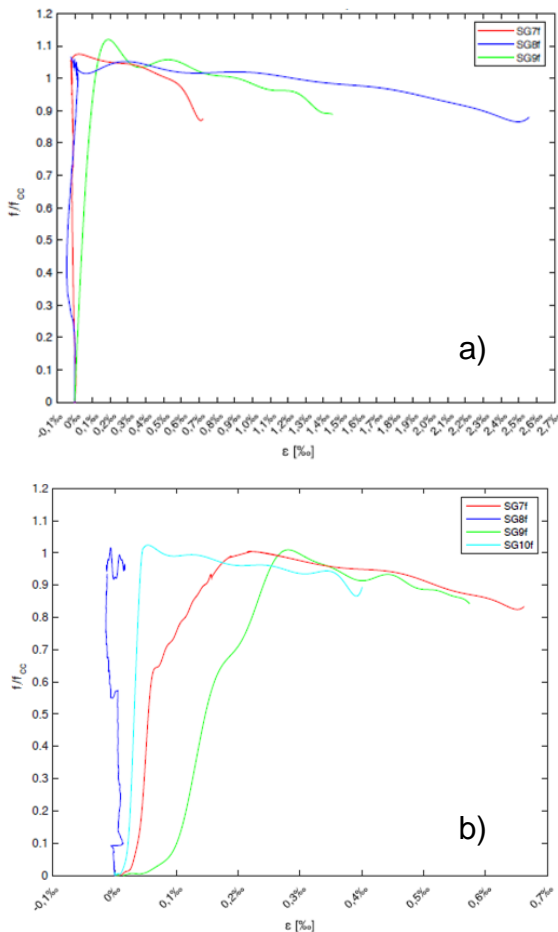


Figure 9. Hoop fiber strain development in: a) C33-2 and b) S33-2 specimens.

CONCLUSIONS

The present paper has shown some recent results about the axial behavior of 1m-height RC columns, jacketed with a carbon-FRCM system, consisting in one or two layers of carbon sheets embedded in a cementitious matrix. The experimental behavior of the test samples has been characterized in terms of global axial stress-strain curve, and then locally transverse strains in the stirrups and hoop fibers were evaluated. The main variables of the experimental campaign were the section geometry, the number of fiber layers and lastly the stirrups spacing.

Results obtained in this work highlighted a significant influence of all the analyzed parameters, that can be resumed as it follows:

- section geometry plays a fundamental role in the ability to fully exploit the properties of the strengthening system. Indeed, even if section edges in square columns were properly rounded, stress concentrations

there hindered the possibility to attain high transverse strains in the fibers.

- the number of fiber layers influences both peak strength and the ultimate strain of the elements. With the increase of this parameter, especially for circular cross-section specimens, the experimental behavior is enhanced.
- for unconfined specimens, those having the lowest stirrups spacing are characterized by the highest peak strength. For the confined ones, among the circular ones, there is a better contribution on the strength gain for those columns having the lowest stirrups spacing; such conclusion seems less pronounced for the squared specimens, at least for those strengthened with one fibers layer only.

ACKNOWLEDGMENT

Authors would like to express their gratitude to MSc Eng. Andrea Dalla Pria and Mirko Pozzato for their help during the execution of the tests. G&P Intech is also acknowledged for providing the FRCM system.

REFERENCES

- Colajanni P., De Domenico F., Recupero A., Spinella N., 2014a. Concrete columns confined with fibre reinforced cementitious mortars: experimentation and modelling. *Constr Build Mater*, **52**, 375-384.
- Colajanni P., Fossetti M., Macaluso G., 2014b. Effects of confinement level, cross-section shape and corner radius on the cyclic behavior of CFRCM confined concrete columns. *Constr Build Mater*, **55**, 379-389.
- De Caso Y Basalo F.J., Matta F., Nanni A., 2012. Fiber reinforced cement-based composite system for concrete confinement. *Constr Build Mater*, **32**, 55-65.
- Gonzalez-Libreros J., Faleschini F., Zanini M.A., Pellegrino C., 2019. Effect of corner radius on the axial behavior of FRCM-confined members, *Rilem Spring Convention and SMSS Conference*, Rovinj, Croatia, 18-22 March 2019.
- Pellegrino C., D'Antino T., 2013. Experimental behaviour of existing precast prestressed reinforced concrete elements strengthened with cementitious composites, *Compos Part B Eng*, **55**, 31-40.
- Tetta Z.C., Bournas D.A., 2016. TRM vs FRP jacketing in shear strengthening of concrete members subjected to high temperatures, *Compos Part B Eng*, **106**, 190-205.
- Triantafillou T.C., Papanicolaou C.G., Zissimopoulos P., Laourdekis T., 2006. Concrete confinement with textile-reinforced mortar jackets, *ACI Struct J*, **103**, 28-37.
- Triantafillou T.C., Papanicolaou C.G., 2006. Shear strengthening of reinforced concrete members with textile reinforced mortar (TRM) jackets. *Mater Struct Constr*, **39**, 93-103.